Title

Posterior Papillary Muscle Anchoring Affects Remote Myofiber Stress and Pump Function: Finite Element Analysis

Journal

The Annals of Thoracic Surgery, 98(4)

ISSN

0003-4975

Authors

Pantoja, Joe Luis
Ge, Liang
Zhang, Zhihong
et al.

Publication Date

2014-10-01

DOI

10.1016/j.athoracsur.2014.04.077

Peer reviewed

HHS Public Access

Author manuscript

Ann Thorac Surg. Author manuscript; available in PMC 2018 July 18.

Published in final edited form as:

Ann Thorac Surg. 2014 October ; 98(4): 1355–1362. doi:10.1016/j.athoracsur.2014.04.077.

Posterior Papillary Muscle Anchoring affects Remote Myofiber Stress and Pump Function: Finite Element Analysis

Joe Luis Pantoja, BS[3], **Liang Ge, PhD**[1,2,4], **Zhihong Zhang, MS**[4], **William G. Morrel, BS**[3], **Julius M. Guccione, PhD**[1,2,4], **Eugene A Grossi, MD**[5,6], and **Mark B. Ratcliffe, MD**[1,2,4]

[1]Department of Surgery, University of California, San Francisco, California

[2]Department of Bioengineering, University of California, San Francisco, California

[3]University of California, San Francisco, California

[4]Veterans Affairs Medical Center, San Francisco, California

[5]Department of Cardiothoracic Surgery, New York University

[6]New York Harbor Veterans Affairs Medical Center, New York, New York

Abstract

Objectives—The role of posterior papillary muscle anchoring (PPM/PPMA) in the management of chronic ischemic functional mitral regurgitation is controversial. We studied the effect of anchoring point direction and relocation displacement on left ventricular (LV) regional myofiber stress and pump function.

Methods—Previously described finite element models of sheep 16 weeks after postero-lateral myocardial infarction (MI) were used. True-sized mitral annuloplasty (MA) ring insertion plus different PPM anchoring techniques were simulated. Anchoring points tested included both commissures and the central anterior mitral annulus; relocation displacement varied from 10% to 40% of baseline diastolic distance from the PPM to the anchor points on the annulus. For each reconstruction scenario, myofiber stress in the MI, borderzone, and remote myocardium and pump function were calculated.

Results—PPMA caused reductions in myofiber stress at end-diastole and end-systole in all regions of the LV that were proportional to the relocation displacement. While stress reduction was greatest in the MI region, it also occurred in the remote region. The maximum 40% displacement caused a slight reduction in LV pump function. However, with the correction of regurgitation by MA plus PPMA, there was an overall increase in forward stroke volume. Finally, anchoring point direction had no effect on myofiber stress or pump function.

Conclusion—PPMA reduces remote myofiber stress which is proportional to the absolute distance of relocation and independent of anchoring point. Aggressive use of PPMA techniques to reduce remote myofiber stress may accelerate reverse LV remodeling without impairing LV function.

Corresponding Author: Mark Ratcliffe, Surgical Service (112), San Francisco Veterans Affairs Medical Center, 4150 Clement Street, San Francisco, California 94121. Telephone: (415) 221-4810 x 2962. FAX: (415) 750-2181. mark.ratcliffe@med.va.gov.

Keywords

Finite Element; Mitral Regurgitation; Mitral valve repair; Myocardial Mechanics; Myocardial Remodeling

Introduction

Chronic ischemic functional mitral regurgitation (FMR) is caused by left ventricular (LV) remodeling that occurs typically after postero-lateral myocardial infarction (MI). FMR is a significant problem causing congestive heart failure and deceased survival. [1–3]

The standard surgical treatment for FMR is reduction mitral annuloplasty (MA). Although patients with unrepaired mild to moderate FMR are at increased risk of repeat hospitalization and death [4], the efficacy of MA at the time of coronary bypass (CABG) remains unclear. The Randomized Ischemic Mitral Evaluation trial was stopped early with a greater improvement in peak oxygen consumption in the CABG + MA group [5] and a National Institute of Health sponsored trial of CABG +/− MA for patients with moderate FMR is underway.

However, FMR repair with reduction MA may have an associated re-occurrence in up to 32% of patients. [6–8] These failures are due to the progressive LV enlargement with further displacement of the posterior papillary muscle (PPM) [7]. Therefore, while reduction annuloplasty may be able to initially correct MR, it may not stop or reverse negative LV remodeling particularly in larger ventricles. [9, 10]

As a consequence, a number of ‘subvalvular’ procedures have been proposed. PPM stabilization has been advocated by proponents of papillary muscle banding {Hvass, 2003 #17859} while others have favored anchoring the PPM to anterior ventricular structures. Examples include: 1) a suture placed between the PPM and the right posterior mitral annulus as proposed by Kron [11], 2) a suture between the PPM and the right fibrous trigone region of the anterior mitral annulus as described by Langer et al [12], or 3) between the lateral and anterior LV walls as is the case with the Coapsys LV reshaping device. [13] While it is believed that these procedures acutely reshape the LV and provide long-term stabilization, it is unknown whether they provide remote myofiber stress reduction.

This study uses validated finite element models of the ovine mitral apparatus and ventricle to quantify the acute effects of various PPM relocation techniques. Specifically, the different techniques of anchor point location and the amount of displacement (relocation distance) were studied. We hypothesized that greater PPM displacement and anchoring at the anterior commissure would produce the greatest decreases in remote myofiber stress.

Methods

Animals used in this study were treated in compliance with the “Guide for the Care and Use of Laboratory Animals”. Five male adult Dorset sheep underwent postero-lateral MI as previously described [14] with MRI obtained at 16 weeks after MI allowing construction of

five finite element models as previously reported. [15–16] LV myocardium was divided into MI, borderzone (BZ) and remote myocardium, where the BZ-Remote boundary was defined as the point where wall thickness is 70% of the maximum LV wall thickness. The mitral apparatus was simply modeled as described by Wenk. [17, 18] Mitral leaflets were modeled using B-spline curves that estimated leaflet contours. Edge chords were attached to the free edge of each leaflet and strut chords to the mid-section of each leaflet (Figure 1). To isolate the MV apparatus from boundary condition interactions, the basal myocardial nodes were extended above the MV plane and basal epicardial nodes fully constrained. Simulations were performed on a Linux cluster.

Loading and Constitutive Models—The endocardial wall was loaded to the measured *in-vivo* end-diastolic and end-systolic LV pressures. The mitral leaflets were loaded with a pressure of −1.125 mmHg to simulate a pressure gradient from the left atrium to LV throughout diastole. To simulate an outward pressure from the LV, leaflets were loaded with measured in-vivo end-systolic LV pressures throughout systole. Active and passive myocardial constitutive laws, previously described by Guccione [19, 20], were implemented using a user defined material subroutine (LS-DYNA, LSTC, Livermore, CA). Passive stiffness and contractility material properties were optimized to match end-diastolic and end-systolic volumes of each animal specific finite element model to its respective experimental volumes. Average material parameters and comparison of individual model and matched experiment are detailed in Appendix A. The MV leaflets and aortic root cap were modeled with LS-DYNA material properties for soft tissue (*MAT_091) while the chordae tendineae were modeled with cable elements (*MAT_071).

Posterior Papillary Muscle Anchoring—PPM anchoring was performed using a virtual suture method with the suture modeled as a cable beam carrying a predefined tension with a Young's modulus of $E=1.0 \times 10^6$ kPa to minimize stretching. The anchor was attached to the four surface nodes closest to the chordal attachment of the PPM. The other end of the anchor was either the anterior (AC) and posterior commissure (PC), or the center point (CP) along the anterior annulus (Figure 1). The relocation distance ranged from 10% to 40% of the unshortened diastolic length of the anchor suture.

Mitral Annuloplasty—Virtual MA was performed as previously described. [22] Briefly, a saddle shaped MA ring (Physio II, size 24, Edwards Lifesciences Co., Irvine, CA) was modeled from B-spline curves and true sized for each sheep by scaling to the commissure-to-commissure distance. 32 virtual sutures were evenly placed between the ring and mitral annulus (Figure 2) with axial tensioning effectively drawing the mitral annulus towards the ring.

Measured Outcomes—After each simulated condition, the septal-lateral (SLSA) and anterior-posterior (APSA) short axes were measured at end-systole. Additionally, the distance vector from the PPM to the posterior commissure (PPM->PC) and it's directional components were measured. Regional myocardial fiber stresses in MI, BZ, and remote myocardium were calculated; additional representative sections of the remote myocardium (anterior (RZ-A), septal (RZ-S), and lateral (RZ-L)) were analyzed. The mitral leaflet

coaptation depth was measured as the distance from the MV plane to the top of the coaptation zone. Finally, stroke volume was measured.

Statistical analysis—All values are expressed as mean ± standard deviation and compared by repeated measures analysis using a mixed model to test for both fixed and random effects (PROC MIXED, SAS system for Windows Version 9.3, SAS Institute, Cary, NC). The impacts of anchoring point, displacement, and an interaction factor were tested on myofiber stress (systolic and diastolic) and stroke volume. Displacement was tested as either proportional or absolute PPM displacement. The animal was held as a random variable and the MA case for each sheep was used as a control. Significance was set at $p<0.05$.

Results

Posterior Papillary Muscle Anchoring – Direction and Distance

Baseline PPM->PC diastolic distances were 2.64±0.61 cm, 1.52±0.58 cm, and 1.05±0.58 cm in the basal-apical, anterior-posterior, and septal-lateral directions respectively. All tested conditions resulted in a basal, septal, and anterior relocation of the PPM towards the mitral annulus ($F=35.16$, $F=33.17$, $F=14.55$, $p<0.0001$ for all, respectively). The AC direction had the greatest basal and anterior displacements, while the central anterior annulus direction had the greatest septal displacement (Figure 3).

Effect on LV Shape

All PPM relocations with displacements greater than 10% decreased SLSA compared to MA ($F=6.56$, $p<0.0001$) (Figure 3). Furthermore, SLSA decreased with increasing displacement ($F=13.36$, $p<0.0001$) and was weakly associated to anchoring direction ($F= 3.20$, $p=0.0505$), with the CP anchor point causing the greatest SLSA decrease. APSA did not decrease compared to MA ($F=0.27$, $p=0.9934$) and was not correlated to changes in anchor point ($F=0.69$, $p=0.5065$) nor displacement ($F=0.05$, $p=0.9843$).

Effect on Regional Myofiber Stress

Regional myocardial stress at end-diastole and end-systole significantly decreased with all displacement and anchor point combinations except 10% displacement, compared to the MA (Figure 4). Furthermore, myofiber stress reductions varied regionally with maximal PPM displacement affecting the MI region the most (Diastolic: 1.3936±0.2399kPa, Systolic: 8.6659+/−1.3140 kPa) and the remote myocardium the least (Diastolic: 0.09805±0.0094kPa, Systolic:1.0259+/−0.1242 kPa). Regional myofiber stress was significantly decreased by increasing displacement ($p<0.0001$ in all regions). However, significance was lost when controlling for SLSA (MI: $p=0.8168$, borderzone: $p=0.9953$, Remote: $p=0.3737$), while SLSA was significantly correlated to myofiber stress (MI: $F=35.96$, $p<0.0001$, borderzone: $F=13.95$, $p=0.0005$, Remote: $F=33.95$, $p<0.0001$). Therefore, decreasing SLSA, which was achieved through PPMA, was the direct mediating factor in myofiber stress reduction and not displacement. Anchor point location also affected regional myofiber stress (MI: $p=0.0028$, borderzone: $p=0.0010$, Remote: $p=0.0004$). However, significance was lost after controlling for absolute displacement (instead of % displacement) (MI: $p=0.5996$, borderzone: $p=0.5054$, Remote: $p=0.998$). With maximal PPM displacement, peak systolic

and diastolic changes in stress in remote regions were decreases of 11.03% and 23.38% for RZ-A, 3.60% and 4.93% for RZ-L, and increases of 2.11% and 5.22% for RZ-S, respectively.

Effect on Mitral Leaflet Position

All PPMA scenarios with displacements greater than 10% reduced coaptation depth, compared to MA ($F=9.38$, $p<0.0001$) (Figure 5). There was a significant reduction in coaptation depth with increasing displacement ($F=25.68$, $p<0.0001$), with 40% displacement causing the coaptation zone to move 0.25+/0.14cm above the annular plane. Lastly, anchor point location was not associated with changes in coaptation depth ($F=0.05$, $p=0.9541$).

Effect on Pump Function

All PPMA scenarios with displacements greater than 10% significantly reduced end-diastolic ($F=35.32$, $p<0.0001$) and end-systolic volumes ($F=24.92$, $p<0.0001$) compared to MA (Figure 6A and B). Additionally, only scenarios with a maximal 40% displacement caused a significant reduction in stroke volume ($F=6.83$, $p<0.0001$). However, if correction of FMR by MA + PPMA is assumed to prevent regurgitant volume (Table 2), there was an overall increase in forward stroke volume (Figure 6C).

Since PPMA procedures by definition reduce ventricular volume, the effects on stroke volume were measured after controlling for end-diastolic and end-systolic volumes. The effects of displacement on stroke volume were statistically insignificant after controlling for end-diastolic volume ($F=1.58$, $p=0.2174$). Lastly, anchor point location had no significant effect on stroke volume ($F=0.61$, $p=0.5496$), end-diastolic volume ($F=1.24$, $p=0.2987$), nor end-systolic volume ($F=0.24$, $p=0.7877$) after controlling for absolute displacement.

Discussion

The principal finding of this study is that PPM anchoring causes a reduction in myofiber stress at end-diastole and end-systole in MI, borderzone and remote regions of the LV that is proportional to the percentage displacement but independent of anchor point location.

Anchor Point Direction—Anchor point location affected myofiber stress when the degree of PPMA is measured as a proportional displacement, but did not reduce stress when PPMA is measured as an absolute displacement. In other words, the absolute distance of PPM displacement was more important than the direction to which it was drawn. That anchor point affects both the magnitude and direction of PPM displacement has implications for mitral valve function and FMR. This was demonstrated most clearly in the study by Langer and colleagues in which PPMA relocation towards the posterior and anterior commissures alone and combination was studied in sheep. [23] In their series, only PPMA to the posterior commissure caused displacement of the PPM toward the mitral annulus. [23] Although Langer adjusted PPMA suture tension in this and subsequent studies to observed effect [12, 23], it appears that his relocation corresponds approximately to only our 10% displacement data.

Reductions in Regional Myofiber Stress—There is no consensus in animal and clinical studies about the ability of mitral valve repair to reverse the LV remodeling that occurs with CIMR. Matsuzaki et al found that mitral annuloplasty does not affect remodeling when performed 8 weeks after postero-lateral MI in sheep. [24] On the other hand, Beeri et al demonstrated return to baseline LV volume when left atrial to LV shunt (MR equivalent) was occluded 6 weeks after MI. [25] While LV size and ejection fraction are significantly improved in patients with CIMR that are treated with CABG + MV repair [26], mortality is not improved. [27, 28]

Left ventricular enlargement (remodeling) after myocardial infarction is a consequence of infarct expansion, extension of the infarct borderzone [29], hypertrophy of the remote myocardium, and the effects of neuro-humoral compensatory pathways. [30] Of those, infarct expansion, borderzone extension and remote zone changes are thought to be mediated by wall stress. It is possible that, when PPMA mediated reduction in stress is added to the reduction in end-diastolic stress that occurs when the mitral valve becomes competent, LV reverse remodeling (reduction in LV volume) will accelerate after mitral repair for CIMR.

The mediocre post-operative stress reductions mediated by reductions in SLSA observed in our study may also account for the unique improved mortality observed in the RESTORE-MV trial of the Coapsys device. [31] In a recent finite element study of the Coapsys device, the increase in 1-year survival rate with Coapsys compared to MA was posulated to be attributable to the sizable stress reduction achieved after ventricular shape change. [32] Significantly and unfortunately, PPMA in this experimental series did not effect major changes in LV geometry vis-a-vie remote myocardial stress reduction as demonstrated with Coapsys reshaping, where reductions in 53% in diastole and 32% in systole were noted. This is at least an order of magnitude greater than the 9% diastolic 7% systolic changes in remote myocardial stress noted here by pulling on the PM tip. Whether a more radical papillary muscle and injured ventricular wall reshaping will produce more favorable remote myocardial stress changes is unknown and should be the subject of future investigations.

Effect on Mitral Valve Geometry—What this study does affirm are the favorable leaflet changes which result in improved coaptation depth. The coaptation depth or ‘tenting’ of the repaired valves clearly decreased proportionately with PPM displacement. As reconfirmed in the recent CTSN study of CIMR surgery [6], recurrent MR remains a significant issue with a repair strategy; it was present in 32.6% of survivors (28.4% moderate and 4.2% severe) at one year. Unfortunately no information regarding the baseline ventricular dimensions in the ‘recurring’ patients was given. We could speculate that the decrease in tenting depth associated with PPMA might decrease the incidence of recurrent MR in this vulnerable population. The unresolved issue is whether these changes will persist and help reduce recurrent MR. If they are only temporary, those ventricles with significant ventricular injury will continue to negatively remodel, disrupting a repair and producing recurrent MR. The degree of long-term ‘resiliency’ PPMA clinically adds to a FMR repair remains unknown.

Effect on Pump Function—PPMA in which anchor point to PPM distance was reduced by 40% caused a slight reduction in LV pump function. Although PPMA reduced both ESV

and EDV, the reduction in stroke volume was primary driven by EDV. This is similar to the reduction in pump function in other procedures that reshape the LV [33] and in LV volume reduction procedures [34], However, as with the Coapsys device [32], if correction of CIMR by MA + PPMA is assumed, there was an overall increase in forward stroke volume.

Study Limitations

Several assumptions were incorporated into the model. Firstly, the fiber direction was uniform throughout the papillary muscle (aligned to the apical-basal direction) and based on the previous computational models. [17] The central surface of the PPM bodies were used as chordal attachment points; finer modeling of the papillary trunks was not available. Furthermore, the finite element model did not incorporate fluid-structure interactions. Thus, the surgical effects on regurgitant volumes were not directly measured. It was assumed that MA and PPMA successfully eliminated MR. Pre-op regurgitant volumes were estimated as the in vivo difference between left and right ventricular SV.

Conclusions and Future Directions

PPMA causes a reduction in myofiber stress in all regions of the LV that is proportional to the degree of tightening; with only small reductions noted in the remote myocardium. It is unknown whether such modest remote stress reductions may arrest or mitigate negative LV remodeling. PPMA does improve leaflet tethering, but its persistence and potential to diminish recurrent MR is unknown. With variations in PPMA procedures and few systematic investigations, virtual surgery methodology will continue to provide procedural analysis and allow for optimization of strategies.

Acknowledgments

This study was supported by NIH grant R01-HL-63348 (Dr. Ratcliffe) and by AHA grant 13MSRF17090108. This support is gratefully acknowledged.

Abbreviations

AC	Anterior Commissure
APSA	Anterior-Posterior Short Axis
BZ	Borderzone
CABG	Coronary Artery Bypass Graft
CP	Center Point
FMR	Functional Mitral Regurgitation
LV	Left Ventricle
MI	Myocardial Infarction
MA	Mitral Annuloplasty

PC	Posterior Commissure
PPM	Posterior Papillary Muscle
PPM->PC	Distance Vector from the PPM to the Posterior Commissure
PPMA	Posterior Papillary Muscle Anchoring
RZ-A	Anterior Remote Zone
RZ-L	Lateral Remote Zone
RZ-S	Septal Remote Zone
SLSA	Septal-Lateral Short Axis

References

1. Heart disease and stroke statistics: 2006 update American Heart Association; 2006
2. Gorman RC, , Gorman JH, , 3rd, Edmunds LH, Jr. Ischemic mitral regurgitation in cardiac surgery in the adult. In: Cohn LH, , Edmunds LH, Jr, editorsCardiac Surgery in the adult McGraw-Hill; New York: 2003 175170
3. Massie BM, Packer M. Congestive heart failure. Current controversies and future prospects. Am J Cardiol. 1990; 66:429.
4. Schroder JN, Williams ML, Hata JA, Muhlbaier LH, Swaminathan M, Mathew JP, et al. Impact of mitral valve regurgitation evaluated by intraoperative transesophageal echocardiography on long-term outcomes after coronary artery bypass grafting. Circulation. 2005; 112(9 Suppl):I293–8. [PubMed: 16159834]
5. Chan KM, Punjabi PP, Flather M, Wage R, Symmonds K, Roussin I, et al. Coronary artery bypass surgery with or without mitral valve annuloplasty in moderate functional ischemic mitral regurgitation: final results of the Randomized Ischemic Mitral Evaluation (RIME) trial. Circulation. 2012; 126(21):2502–10. [PubMed: 23136163]
6. Acker MA, Parides MK, Perrault LP, Moskowitz AJ, Gelijns AC, Voisine P, et al. Mitral-Valve Repair versus Replacement for Severe Ischemic Mitral Regurgitation. N Engl J Med. 2013
7. De Bonis M, Lapenna E, Verzini A, La Canna G, Grimaldi A, Torracca L, et al. Recurrence of mitral regurgitation parallels the absence of left ventricular reverse remodeling after mitral repair in advanced dilated cardiomyopathy. Ann Thorac Surg. 2008; 85(3):932–9. [PubMed: 18291174]
8. Matsunaga A, Tahta SA, Duran CM. Failure of reduction annuloplasty for functional ischemic mitral regurgitation. J Heart Valve Dis. 2004; 13(3):390–7. discussion 397–8. [PubMed: 15222285]
9. Braun J, Bax JJ, Versteegh MIM, Voigt PG, Holman ER, Klautz RJM, et al. Preoperative left ventricular dimensions predict reverse remodeling following restrictive mitral annuloplasty in ischemic mitral regurgitation ☆. European Journal of Cardio-Thoracic Surgery. 2005; 27(5):847–853. [PubMed: 15848325]
10. Magne J, Pibarot P, Dagenais F, Hachicha Z, Dumesnil JG, Senechal M. Preoperative posterior leaflet angle accurately predicts outcome after restrictive mitral valve annuloplasty for ischemic mitral regurgitation. Circulation. 2007; 115(6):782–91. [PubMed: 17283262]
11. Kron IL, Green GR, Cope JT. Surgical relocation of the posterior papillary muscle in chronic ischemic mitral regurgitation. Ann Thorac Surg. 2002; 74(2):600–1. [PubMed: 12173864]
12. Langer F, Kunihara T, Hell K, Schramm R, Schmidt KI, Aicher D, et al. RING+STRING: Successful repair technique for ischemic mitral regurgitation with severe leaflet tethering. Circulation. 2009; 120(11 Suppl):S85–91. [PubMed: 19752391]
13. Grossi EA, Woo YJ, Schwartz CF, Gangahar DM, Subramanian VA, Patel N, et al. Comparison of Coapsys annuloplasty and internal reduction mitral annuloplasty in the randomized treatment of functional ischemic mitral regurgitation: impact on the left ventricle. J Thorac Cardiovasc Surg. 2006; 131(5):1095–8. [PubMed: 16678595]

14. Llaneras MR, Nance ML, Streicher JT, Lima JA, Savino JS, Bogen DK, et al. Large animal model of ischemic mitral regurgitation. Ann Thorac Surg. 1994; 57(2):432–9. [PubMed: 8311608]
15. Soleimani M, Khazalpour M, Cheng G, Zhang Z, Acevedo-Bolton G, Saloner DA, et al. Moderate mitral regurgitation accelerates left ventricular remodeling after posterolateral myocardial infarction. Ann Thorac Surg. 2011; 92(5):1614–20. [PubMed: 21945222]
16. Shimkunas R, Zhang Z, Wenk JF, Soleimani M, Khazalpour M, Acevedo-Bolton G, et al. Left ventricular myocardial contractility is depressed in the borderzone after posterolateral myocardial infarction. Ann Thorac Surg. 2013; 95(5):1619–25. [PubMed: 23523189]
17. Wenk JF, Zhang Z, Cheng G, Malhotra D, Acevedo-Bolton G, Burger M, et al. First finite element model of the left ventricle with mitral valve: insights into ischemic mitral regurgitation. Ann Thorac Surg. 2010; 89(5):1546–53. [PubMed: 20417775]
18. Wenk JF, Ratcliffe MB, Guccione JM. Finite element modeling of mitral leaflet tissue using a layered shell approximation. Med Biol Eng Comput. 2012
19. Guccione JM, McCulloch AD, Waldman LK. Passive material properties of intact ventricular myocardium determined from a cylindrical model. J Biomech Eng. 1991; 113(1):42–55. [PubMed: 2020175]
20. Guccione JM, Waldman LK, McCulloch AD. Mechanics of active contraction in cardiac muscle: Part II--Cylindrical models of the systolic left ventricle. J Biomech Eng. 1993; 115(1):82–90. [PubMed: 8445902]
21. Sun K, Stander N, Jhun CS, Zhang Z, Suzuki T, Wang GY, et al. A computationally efficient formal optimization of regional myocardial contractility in a sheep with left ventricular aneurysm. J Biomech Eng. 2009; 131(11):111001. [PubMed: 20016753]
22. Wong VM, Wenk JF, Zhang Z, Cheng G, Acevedo-Bolton G, Burger M, et al. The effect of mitral annuloplasty shape in ischemic mitral regurgitation: a finite element simulation. Ann Thorac Surg. 2012; 93(3):776–82. [PubMed: 22245588]
23. Langer F, Rodriguez F, Ortiz S, Cheng A, Nguyen TC, Zasio MK, et al. Subvalvular repair: the key to repairing ischemic mitral regurgitation? Circulation. 2005; 112(9 Suppl):I383–9. [PubMed: 16159851]
24. Matsuzaki K, Morita M, Hamamoto H, Noma M, Robb JD, Gillespie MJ, et al. Elimination of ischemic mitral regurgitation does not alter long-term left ventricular remodeling in the ovine model. Ann Thorac Surg. 2010; 90(3):788–94. [PubMed: 20732497]
25. Beeri R, Yosefy C, Guerrero JL, Nesta F, Abedat S, Chaput M, et al. Mitral regurgitation augments post-myocardial infarction remodeling failure of hypertrophic compensation. J Am Coll Cardiol. 2008; 51(4):476–86. [PubMed: 18222360]
26. Prifti E, Bonacchi M, Frati G, Giunti G, Babatasi G, Sani G. Ischemic mitral valve regurgitation grade II–III: correction in patients with impaired left ventricular function undergoing simultaneous coronary revascularization. J Heart Valve Dis. 2001; 10(6):754–62. [PubMed: 11767182]
27. Diodato MD, Moon MR, Pasque MK, Barner HB, Moazami N, Lawton JS, et al. Repair of ischemic mitral regurgitation does not increase mortality or improve long-term survival in patients undergoing coronary artery revascularization: a propensity analysis. Ann Thorac Surg. 2004; 78(3):794–9. discussion 794–9. [PubMed: 15336993]
28. Kim YH, Czer LS, Soukiasian HJ, De Robertis M, Magliato KE, Blanche C, et al. Ischemic mitral regurgitation: revascularization alone versus revascularization and mitral valve repair. Ann Thorac Surg. 2005; 79(6):1895–901. [PubMed: 15919280]
29. Jackson BM, Gorman JH, Moainie SL, Guy TS, Narula N, Narula J, et al. Extension of borderzone myocardium in postinfarction dilated cardiomyopathy. J Am Coll Cardiol. 2002; 40(6):1160–7. discussion 1168–71. [PubMed: 12354444]
30. Bristow MR. The adrenergic nervous system in heart failure. N Engl J Med. 1984; 311(13):850–1. [PubMed: 6472388]
31. Grossi E, Patel N, Woo Y, Goldberg J, Schwartz C, Subramanian V, et al. Outcomes of the Randomized Evaluation of a Surgical Treatment for Off-pump Repair of the Mitral Valve (RESTOR-MV) Trial. J Am Coll Cardiol. 2010; 55(suppl 1):E1366.

32. Carrick R, Ge L, Lee LC, Zhang Z, Mishra R, Axel L, et al. Patient-specific finite element-based analysis of ventricular myofiber stress after Coapsys: importance of residual stress. Ann Thorac Surg. 2012; 93(6):1964–71. [PubMed: 22560323]
33. Guccione JM, Salahieh A, Moonly SM, Kortsmit J, Wallace AW, Ratcliffe MB. Myosplint decreases wall stress without depressing function in the failing heart: a finite element model study. Ann Thorac Surg. 2003; 76(4):1171–80. discussion 1180. [PubMed: 14530007]
34. Zhang P, Guccione JM, Nicholas SI, Walker JC, Crawford PC, Shamal A, et al. Left ventricular volume and function after endoventricular patch plasty for dyskinetic anteroapical left ventricular aneurysm in sheep. J Thorac Cardiovasc Surg. 2005; 130(4):1032–8. [PubMed: 16214516]

Appendix A: Applied Material Properties and Model comparisons

A. Diastolic material parameters bf=49.25 bt=19.25 bfs=17.44 were used for all regions.

B. Regionally Varying Averaged Material Properties:

	Passive Stiffness, C (kPa)	**Contractility, T_{max} (kPa)**
Remote zone	0.0298±0.02	203.05±51.43
Border zone	0.0298±0.02	61.29±17.44
Infarct	0.298±0.23	0±0

C. Comparison between experimental (MRI) and finite element model left ventricular volumes is presented in the table below. Regurgitant volume was estimated as the in-vivo difference between left and right ventricular stroke volumes.

	End Diastolic Volume (mL)	**End Systolic Volume (mL)**	**Stroke Volume (mL)**	**Regurgitant Volume (mL)**
Pre-op MRI Scan	91.56±12.72	52.98±12.2	38.58±5.28	14.4±5.46
Finite Element Pre-op model	92.3±17.09	56.9±10.53	35.4±13.53	N/A

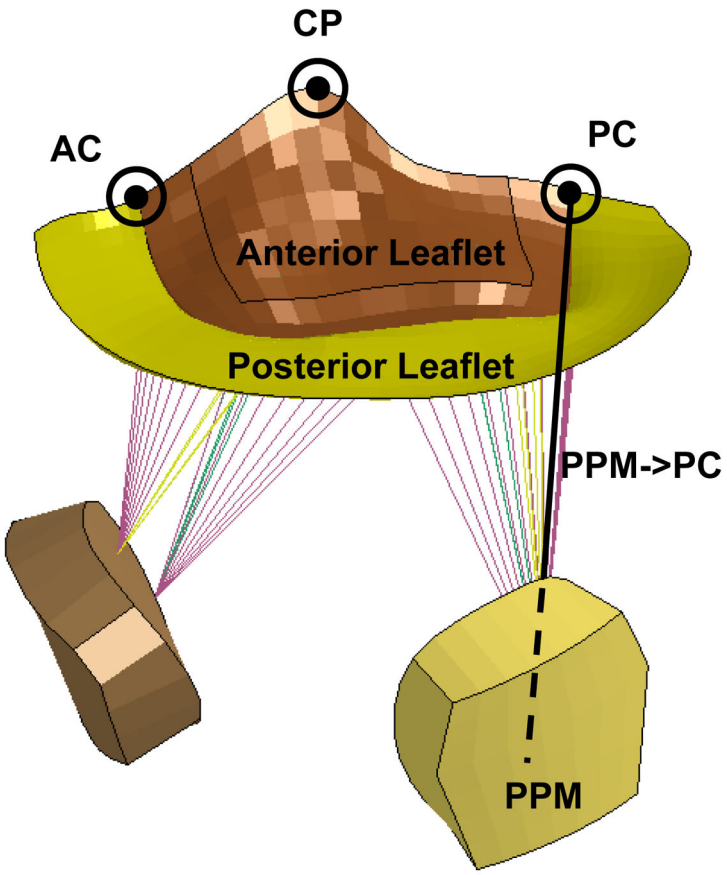

Figure 1.

PPMA suture was placed between the PPM and either the anterior commissure (AC), posterior commissure (PC), or the center (CP) anterior annulus anchor points. The PPM position was tracked by measuring PPM->PC.

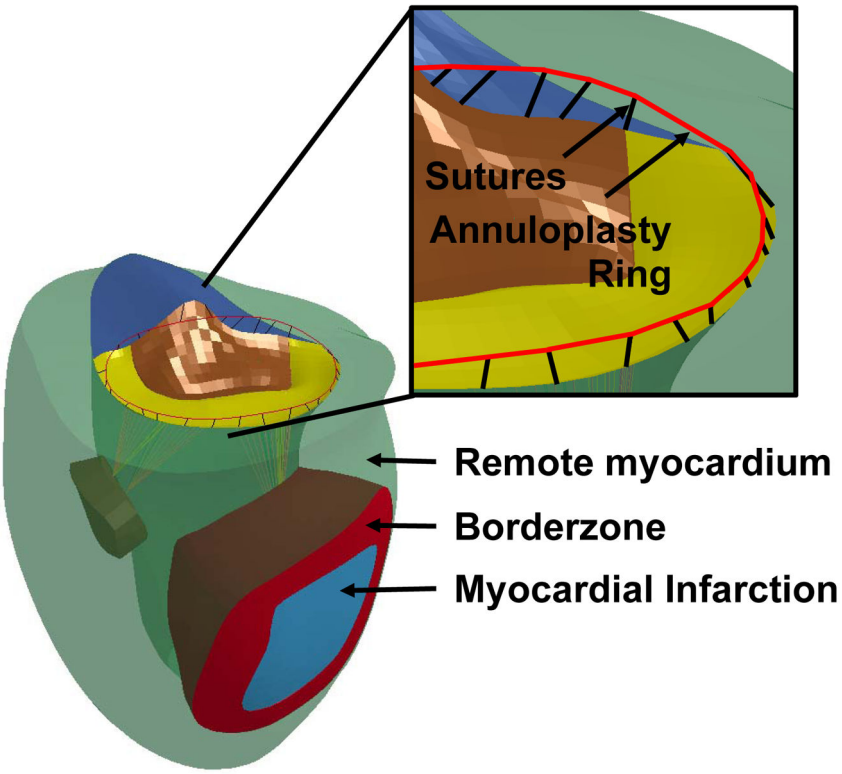

Figure 2.
Diastolic LV model demonstrating the MA ring and suture placements around the mitral annulus

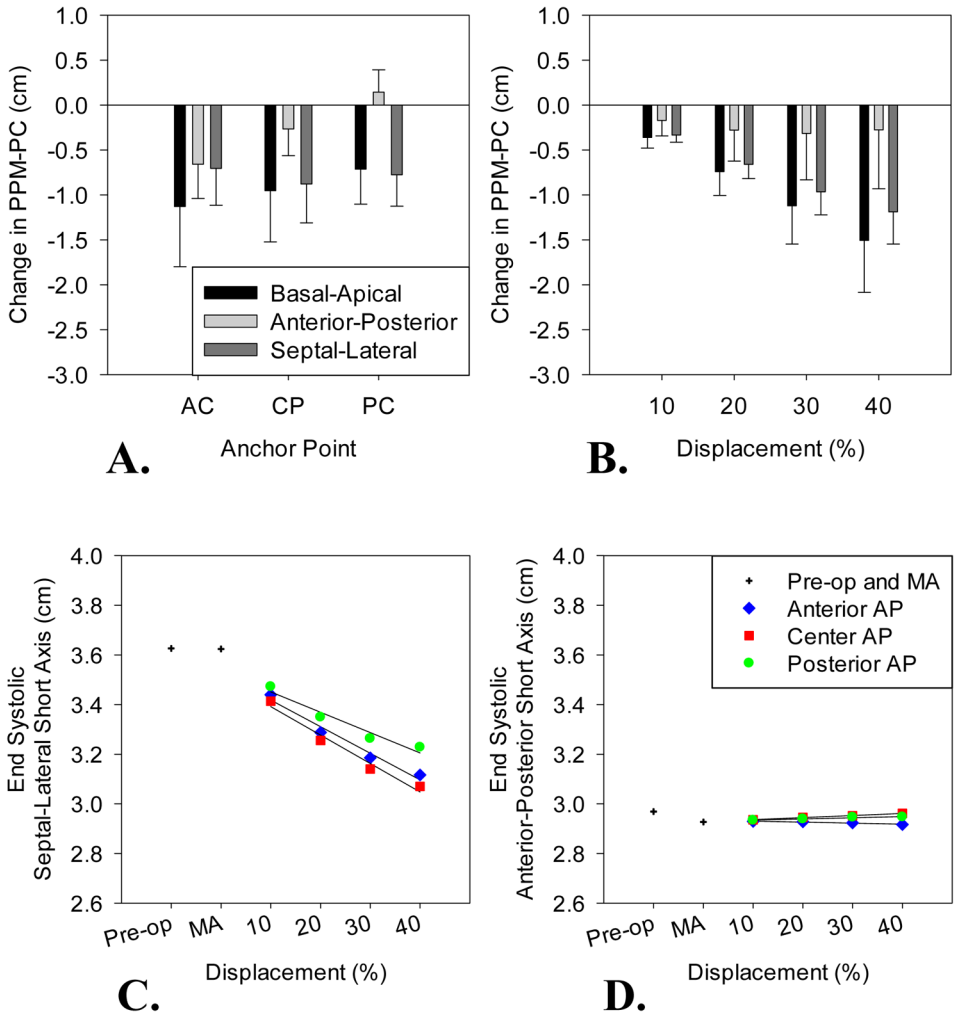

Figure 3.

Effect of anchor point location (A) and displacement (B) on PPM->PC (Differences are with respect to the MA), and Septo-lateral (C), and Anterior-posterior LV Diameter (D).

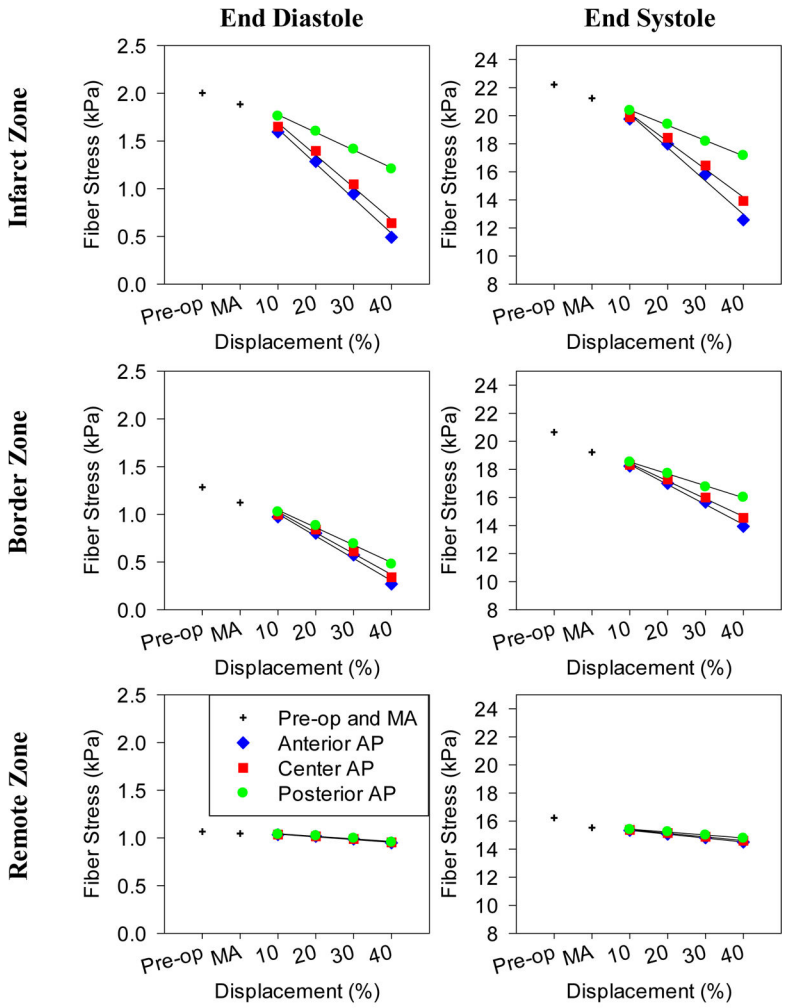

Figure 4.

Effect of anchor point location and displacement on end-diastolic and end-systolic regional myofiber stress (legend applies to all graphs)

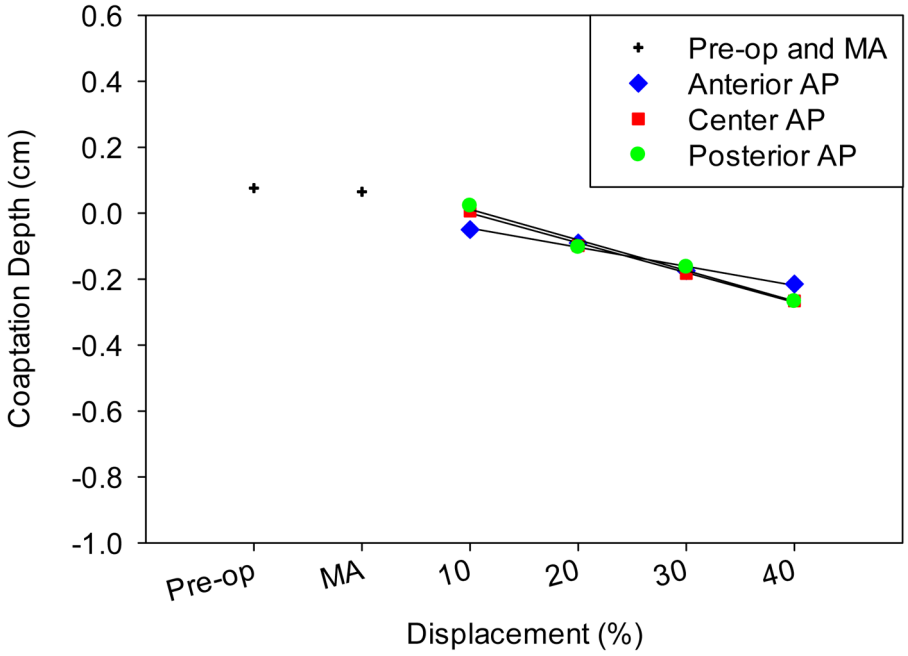

Figure 5.
Effect of anchor point location and displacement on mitral leaflet coaptation depth measured from the annular plane to the top of the A2-P2 coaptation zone

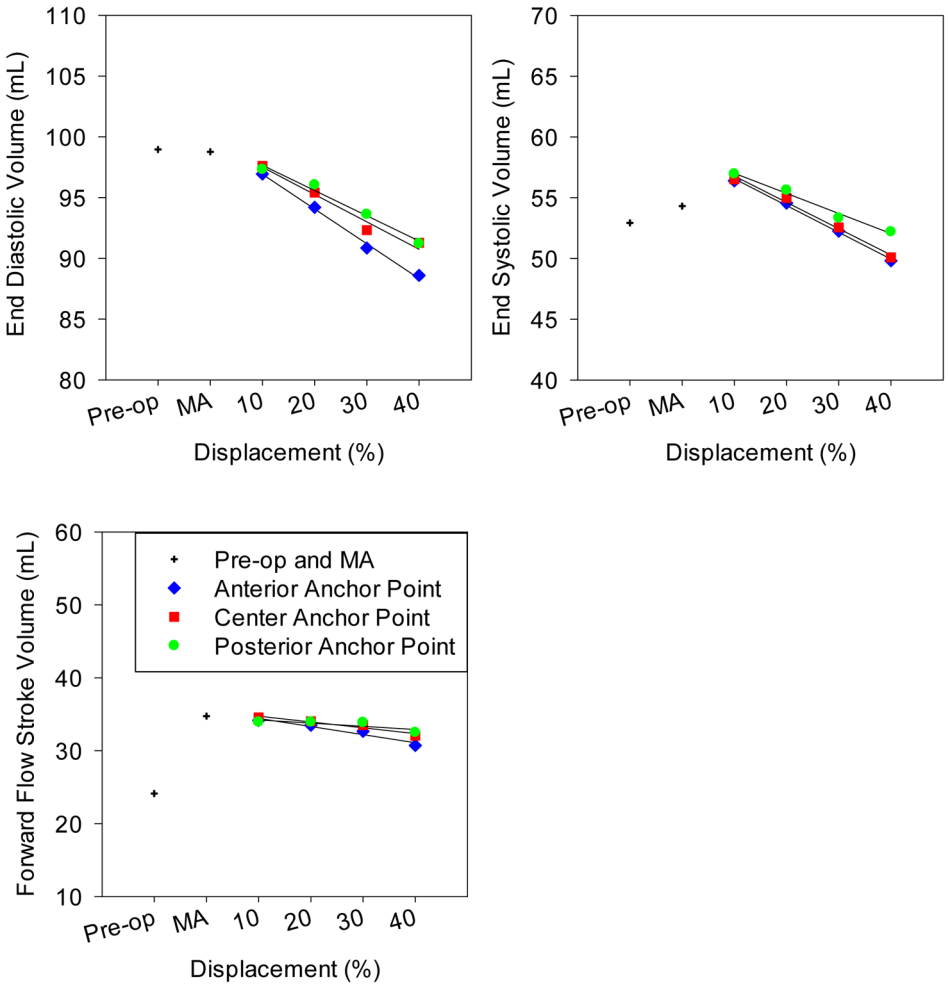

Figure 6.

Effect of anchor point location (A) and displacement (B) on end-diastolic, end-systolic, and stroke volumes (legend applies to all graphs)